

## Nonclassical Excitation for Atoms in a Squeezed Vacuum

N. Ph. Georgiades, E. S. Polzik,<sup>\*</sup> K. Edamatsu,<sup>†</sup> and H. J. Kimble

*Norman Bridge Laboratory of Physics, California Institute of Technology 12-33, Pasadena, California 91125*

A. S. Parkins<sup>‡</sup>

*Department of Physics, University of Konstanz, Konstanz, Germany*

(Received 21 April 1995)

The two-photon transition  $6S_{1/2} \rightarrow 6D_{5/2}$  is investigated for trapped atomic cesium excited by squeezed light. The rate  $R$  of two-photon excitation versus intensity  $I$  is observed to be consistent with the functional form  $R = \beta_1 I + \beta_2 I^2$ , extending into a region with slope 1.3. This departure from the quadratic form for classical light sources is due to the fundamental alteration of atomic radiative processes by the nonclassical field.

PACS numbers: 42.50.Dv, 32.80.-t

Although tremendous progress has been made over the past two decades in the understanding of the generation and application of manifestly quantum or nonclassical states of the electromagnetic field [1–3], there have been until quite recently no frequency tunable sources suitable for spectroscopy. Indeed, throughout its history spectroscopy has been carried out with “classical” sources (typically lasers or thermal fields) in that the Glauber-Sudarshan phase-space function is positive definite. By contrast, spectroscopy with nonclassical light can lead to enhancements in measurement capabilities beyond the usual quantum limits [4] and offers the potential for new optical phenomena associated with fundamental alterations of atomic radiative processes [5]. In fact, by now there is a rather extensive theoretical literature which investigates the phenomenology associated with coupling atoms to nonclassical fields [6].

Against this backdrop, in this Letter we report the first experimental observation of the modification of fundamental atomic radiative processes brought about by illumination with nonclassical light. More specifically, we investigate two-photon atomic excitation, for which the excitation rate  $\Gamma$  can often be expressed in terms of the field correlation function  $C(\tau) = \langle E^\dagger(t + \tau)E^\dagger(t + \tau)E(t)E(t) \rangle$  of the driving field  $E$  [7]. Note that for classical light sources  $\Gamma$  depends quadratically on intensity  $I$  by way of  $C(\tau)$ . By contrast, the manifestly quantum correlations of a squeezed state can enhance this rate such that, for small photon flux,  $\Gamma$  departs from quadratic form and asymptotically becomes a linear function of  $I$  [8–10].

In our experiment squeezed light is generated by nondegenerate parametric down-conversion for excitation of the two-photon transition  $6S_{1/2} \rightarrow 6P_{3/2} \rightarrow 6D_{5/2}$  in atomic cesium. By monitoring fluorescence from  $6D_{5/2} \rightarrow 6P_{3/2}$ , we observe a dependence of excited state population  $\rho_{33}$  on excitation intensity  $I$  that deviates from the quadratic form recorded in our observations with coherent light and that extends into a regime with slope  $\delta \equiv d \log(\rho_{33})/d \log(I) \approx 1.3$ . Furthermore, by employing the measured dependence of excitation

probability on parametric gain  $G$ , we determine that the critical region with slope  $\delta = 1.5$  occurs for  $G \approx 1.4$ . These observations with slope  $\delta < 2$  produce compelling evidence for the nonclassical nature of the excitation process and are supported by a detailed theoretical model.

Turning now to the experimental arrangement as depicted in Fig. 1, we refer first to the atomic levels of the ladder scheme which we denote by  $i = 1, 2, 3$  in correspondence to the  $6S_{1/2}, F = 4$  ground state, the  $6P_{3/2}, F' = 5$  intermediate state (with linewidth 5 MHz FWHM), and the  $6D_{5/2}, F'' = 6$  state (with linewidth 3.2 MHz FWHM) [11], respectively, with transition frequencies  $(\omega_{12}, \omega_{23}, \omega_{13})$  such that  $\omega_{13} = \omega_{12} + \omega_{23}$ . The two-photon transition  $1 \rightarrow 2 \rightarrow 3$  is excited by fields generated via nondegenerate parametric down-conversion at frequencies  $\omega_{\pm}$  symmetrically displaced around the frequency  $\omega_{13}/2 \equiv \omega_0$  (at 883 nm). The overall resonance condition  $\omega_+ + \omega_- = \omega_{13}$  is achieved by a tunable locking scheme of the frequency  $\omega_L$  of a titanium-sapphire (Ti:Al<sub>2</sub>O<sub>3</sub>) laser which optimizes the two-photon excitation rate in the magnetic optical trap (MOT) (as in Fig. 2 of Ref. [11]). With the laser

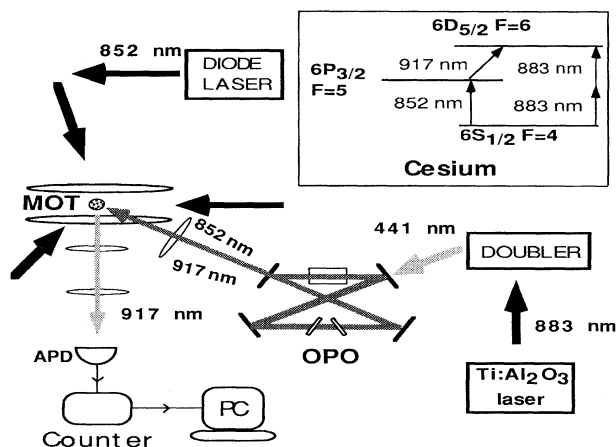


FIG. 1. Experimental arrangement.

frequency thus fixed at  $\omega_L = \omega_0 (\pm 0.3 \text{ MHz})$ , the frequencies  $\omega_{\pm}$  of the signal and idler outputs of the optical parametric oscillator (OPO) are constrained by  $\omega_+ + \omega_- = 2\omega_L$ , since the pump field is simply the frequency-doubled output of the Ti:Al<sub>2</sub>O<sub>3</sub> laser. The condition  $\omega_+ = \omega_{12}$  is identified with an auxiliary semiconductor laser at 852 nm, which is mode matched to and transmitted through the OPO cavity. In the absence of the OPO pump, this laser is focused into the MOT with its frequency set to  $\omega_{12} (\pm 0.3 \text{ MHz})$ . With now the OPO pump present, the incident signal beam at  $\omega_+ = \omega_{12}$  undergoes narrow-band parametric amplification and generates an idler beam at  $\omega_- = \omega_{23}$ .

Of course the gain for this process will be exceedingly small unless the OPO cavity is configured to produce simultaneous resonance for two longitudinal cavity modes at  $\omega_{\pm}$ . Fortunately, the transition frequencies of interest ( $\omega_{12}, \omega_{23}$ ) have a ratio of approximately 14/13. Hence, there will be occasional near overlaps of longitudinal mode resonances around 852 and 917 nm which will approach coincidence as the cavity length is tuned successively through 14 orders for the injected signal field at  $\omega_{12}$ . With the point of optimum gain thus identified for the amplified signal and generated idler fields, the cavity length is fixed by active servo control. By then blocking the injected signal beam, we are left with spontaneous parametric fluorescence around the frequencies  $\omega_+ \approx \omega_{12}$  and  $\omega_- \approx \omega_{23}$ , with overall output flux and spectral properties set by the pump power and the cavity linewidth (FWHM = 8 MHz). Note that the fields at  $\omega_{\pm}$  are strongly correlated, with squeezing of the quadrature amplitudes occurring at an offset of  $\pm 12 \text{ THz}$ .

The output from the OPO is focused with a waist of approximately  $10 \mu\text{m}$  into the MOT, which has a diameter of about  $200 \mu\text{m}$ , and the fluorescence at 917 nm is recorded from the decay  $3 \rightarrow 2$  with an avalanche photodiode (APD). With the trapping beams chopped with a rotating disk at 4 kHz, we define two counting rates  $R_1$  and  $R_2$  corresponding to gated acquisition of fluorescence counts in the intervals with the trapping beams alternatively ON and OFF, respectively. Since in the ON interval the trapping beams provide appreciable population in the level 2 (completely overwhelming the OPO field at  $\omega_+$ ),  $R_1$  provides a measure of the OPO output flux around  $\omega_-$  and hence acts as our surrogate for the excitation intensity. On the other hand, with the trapping beams OFF,  $R_2$  is proportional to the population  $\rho_{33}$  as driven by the combined action of fields at  $\omega_{\pm}$  from the OPO. Hence  $R_2$  vs  $R_1$  has the same functional dependence as does the population  $\rho_{33}$  in level 3 versus incident intensity.

Experimental plots of  $R_2$  vs  $R_1$  for particular runs are shown in Fig. 2, where (a) is taken with squeezed-vacuum excitation, while (b) is acquired with approximate coherent-state excitation [12]. The data in (a) exhibit departure from the usual quadratic form, as made explicit by fitting with the function  $R_2 = \gamma_1 R_1 + \gamma_2 R_1^2$  for which the reduced  $\chi^2$  averages to 1.4 for five most recent runs

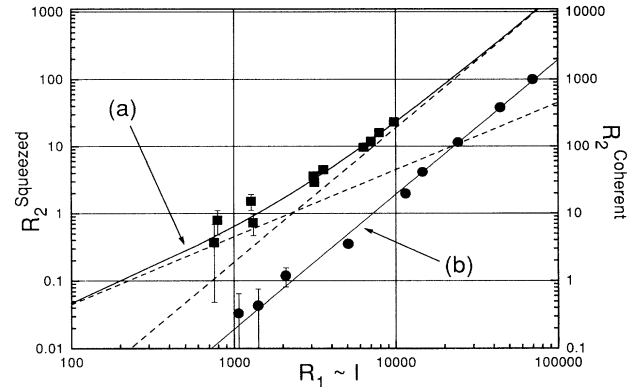


FIG. 2. Excited state population of level 3 due to two-photon transitions ( $R_2$ ) versus excitation intensity ( $R_1$ ), with  $(R_2, R_1)$  as defined in the text. (a) Excitation with squeezed vacuum fit by the functional form  $R_2 = \gamma_1 R_1 + \gamma_2 R_1^2$  with the linear and quadratic components indicated. (b) Excitation with approximately coherent light fit by  $R_2 = a_2 R_1^2$ .

with squeezed excitation. On the other hand, an attempt to fit the same data by a purely quadratic function  $R_2 = \gamma_2 R_1^2$  yields an average reduced  $\chi^2$  of 2.5 for the five runs. Note that in our analysis we assign uncertainties due to statistical errors (arising from Poisson counting fluctuations) and fractional errors (associated with, for example, variations in trap density). We then fit various trial functions  $R_2 = F(R_1)$  to each data set. The significance level for a given  $F$  is then summarized by one of two options. In the first instance we assume that *no additional information* is gained from repeated runs of the experiment and calculate  $\bar{S} = (S_1 \cdot S_2 \cdot \dots \cdot S_5)^{1/5}$ , where  $S_i$  is the significance level for fitting  $F$  to an individual experiment. For a quadratic-plus-linear fit with  $F_{Q+L} = \gamma_2 R_1^2 + \gamma_1 R_1$ , we have  $\bar{S}_{Q+L} = 0.17$ , while for a quadratic fit with  $F_Q = \gamma_2 R_1^2$ , we have  $\bar{S}_Q = 0.004$ . Hence, the probability that the data from any given run are described by a quadratic-plus-linear form exceeds that of a purely quadratic form by a factor of 42. However, because the statistical confidence for several experiments increases beyond the level associated with any one experiment, for the second option we consider the sum of  $\chi^2$  of all the data points from the five runs with squeezed excitation and then calculate the significance levels  $\bar{C}$  for the trial functions. The results are  $\bar{C}_{Q+L} = 0.04$  for a quadratic-plus-linear form, while  $\bar{C}_Q = 5 \times 10^{-10}$  for a quadratic fit. Based on similar analyses we can reject models of the form of a quadratic plus constant,  $F_{Q+C} = aR_1^2 + b$  [for which  $(\bar{S}_{Q+C}, \bar{C}_{Q+C}) = (0.07, 0.001)$ ] and power law  $R_P = cR_1^d$  [for which  $(\bar{S}_P, \bar{C}_P) = (0.05, 0.0006)$ ]. While  $\bar{S}$  clearly underestimates our ability to distinguish between competing hypotheses,  $\bar{C}$  certainly provides an overestimate because of varying systematics from run to run.

By contrast to this situation with squeezed excitation, the data in Fig. 2(b) are well described by a simple quadratic model  $R_2 = \gamma_2 R_1^2$ , as is appropriate for coherent-state

excitation. The reduced  $\chi^2$  for two such experiments averages to 0.96 with associated significance levels, as defined above, of  $(\overline{S}_Q, \overline{C}_Q) = (0.26, 0.37)$ . Therefore, under almost identical experimental conditions, we observe statistically significant differences between the functional forms for two-photon excitation by squeezed-vacuum light versus excitation with coherent light.

Beyond these measurements of  $R_2$  vs  $R_1$ , another avenue for investigating two-photon excitation is provided by the parametric gain  $G$  of the OPO, which is directly related to the statistical properties of the squeezed-vacuum field. Hence, we record not only  $(R_1, R_2)$  but also the OPO gain  $G$  as determined by the amplification of an injected field at 852 nm. The resulting dependence of  $(R_1, R_2)$  on  $G$  is shown on Fig. 3, where the data for  $(R_1, R_2)$  are those of Fig. 2(a). The full curves in the figure are fits by the expressions  $R_1 = \mu_1(G^{1/2} - 1)$  curve (a) and  $R_2 = \nu_1(G^{1/2} - 1) + \nu_2(G^{1/2} - 1)^2$  curve (b), as would be appropriate for an output intensity from the OPO which is proportional to  $G^{1/2} - 1$  and for a dependence of  $R_1$  ( $R_2$ ) on intensity which is linear (linear plus quadratic).

In addition to offering further evidence for a linear component in the two-photon excitation rate, the data of Fig. 3 can be combined with those of Fig. 2(a) to yield another test of the consistency of our procedures and validity of our conclusions. More specifically, we examine the OPO gain  $G_{\text{knee}}$  corresponding to the transition from linear to quadratic regimes, where the ‘‘knee’’ position for the transition is defined to be the point with slope 1.5 from the observed dependence of  $R_2$  vs  $R_1$ . Results are shown in Fig. 4, where in each case (except Exp. 1)  $G_{\text{knee}}$  is determined from measurements of both the amplified signal at 852 nm and the generated idler at 917 nm. The average for these five runs is  $G_{\text{knee}} = 1.36 \pm 0.11$  with reasonable reproducibility, even though there are variations in trap size and density, in focusing geometry, in collection efficiency, and in background levels. This experimental value is to be compared to the theoretical expectation  $G_{\text{knee}} = 1.7$  that is

obtained from numerical integration of the master equation appropriate to our system [13]. At present we have no definitive explanation for the discrepancy between theory and experiment, but numerical simulations indicate that it may be due to small atomic and OPO detunings. Nonetheless, the consistency of measurements of  $G_{\text{knee}}$  offers strong support that the observed functional dependence of  $R_2$  on  $R_1$  is related to the properties of the light emerging from the OPO and not to some spurious effect.

A critical aspect in the measurement of  $R_2$  is the accurate determination of diverse sources of background counts which are typically 5–8/s. Dark counts of the APD (of quantum efficiency 20%) contribute 4/s. Although the detector is shielded by two interference filters centered at 917 nm (with peak transmission of 0.85 each), diffuse scattered light contributes approximately 1/s, while broadband parametric fluorescence escaping from the subthreshold OPO can contribute up to 4/s, but is more typically 0.2/s for alignments that minimize scattering. One of two techniques is used for the background determination for each run. In the first, the magnetic field for the MOT is switched off, thus eliminating the trap; there is no change to any other component of the system, including the OPO. In the second technique, an interference filter for blocking the signal field at 852 nm and transmitting the idler field at 917 nm (with 80% efficiency) is placed in the output path of the OPO, with the trap otherwise unaffected. Within the precision of our data, we can discern no difference in results obtained by these two quite different techniques, which leads us to believe that systematic offsets in the background levels are absent within our quoted uncertainties.

Because our data sets are acquired under conditions that are not constant from run to run, it is difficult to bring the data sets together in one format. However, we can scale our data to the theory by assuming that  $R_1 = k_1 n_{917}$  and  $R_2 = k_2 \rho_{33}$ . Here  $n_{917}$  is the OPO intracavity photon number at 917 nm, while  $\rho_{33}$  is the excited state

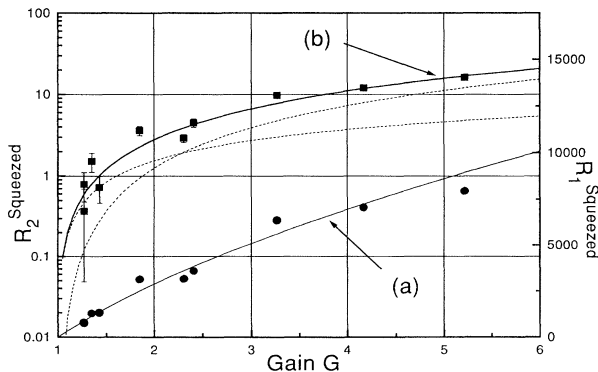


FIG. 3.  $R_1$  [(a) and right-hand scale] and  $R_2$  [(b) and left-hand scale] versus OPO gain  $G$  for squeezed excitation. The full curve (a) corresponds to a linear function of the variable  $G^{1/2} - 1$  while that of curve (b) by a linear plus quadratic function of the same variable with the linear and quadratic components indicated by dashed lines.

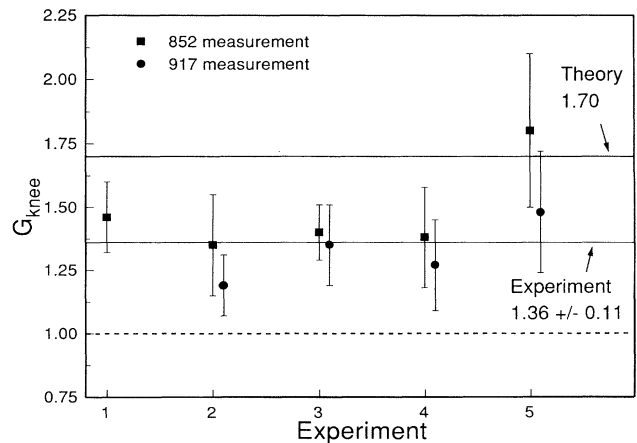


FIG. 4. Parametric gain  $G_{\text{knee}}$  at the position of slope 1.5 for  $R_2$  vs  $R_1$  for different experimental runs.

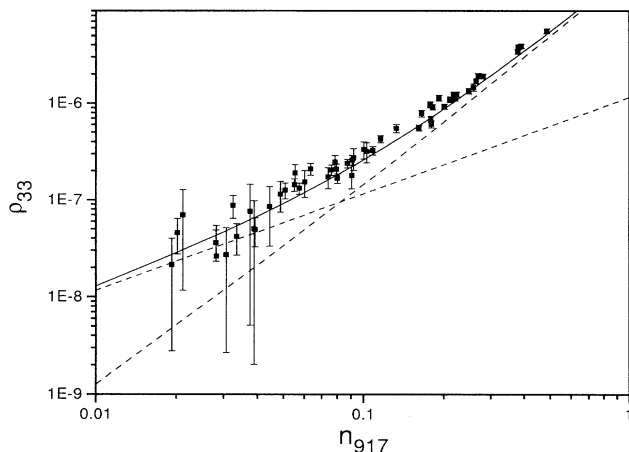


FIG. 5. Level 3 population  $\rho_{33}$  due to two-photon excitation versus intracavity photon number  $n_{917}$  at 917 nm. The counting data ( $R_1, R_2$ ) from five experiments have been scaled as discussed in the text. The full curve is obtained from a numerical solution of the master equation, with the linear and (almost) quadratic components indicated.

population of level 3. The determination of  $k_{1,2}$  is accomplished by means of a least-squares fit to the over-specified system of equations relating the experimentally measured variables  $\{R_1, R_2, G\}$  as in Figs. 2 and 3 to the theoretical variables  $\{\rho_{33}, n_{917}, G\}$ . Figure 5 displays the result of such a procedure applied in turn to the five experiments together with the corresponding theoretical result, with data points in Fig. 5 extending into a region with slope  $< 1.3$ . Note that since the scaling of  $\{R_1, R_2, G\}$  to  $\{\rho_{33}, n_{917}, G\}$  is not *a priori* guaranteed to be internally consistent with the introduction of only two constants  $k_{1,2}$ , the correspondence between experiment and theory evidenced in Fig. 5 favors a fundamental origin for the observed departure from quadratic form. To quantify this point, we calculate  $\bar{C}$  for the scaled data and find that  $\bar{C}_{Q+L} = 0.03$  for a linear-plus-quadratic model. By contrast  $\bar{C}_Q = 2 \times 10^{-10}$  for a purely quadratic model, while  $\bar{C}_{Q+C} = 0.003$  for a quadratic-plus-constant model and  $\bar{C}_P = 0.0002$  for a power law. Although these confidence levels can change significantly for variations of the scaling parameters, the critical point is that  $\bar{C}_{Q+L} \gg (\bar{C}_Q, \bar{C}_{Q+C}, \bar{C}_P)$  for all combinations of the scaling parameters within the allowed error bars.

Given these experimental results and the supporting theory, the question arises as to whether the nonclassical nature of the excitation is a necessary ingredient for producing the observed dependences. Although we know of no proof of complete generality, we can exclude the possibility of a dependence with slope  $\delta < 2$  for classical sources of excitation in several broad cases. In the first place, in situations where the classic result of Mollow applies, namely, that  $\rho_{33}$  follows from  $C(\tau)$ , then the inequality  $|M|^2 < N^2$  ensures that the slope of  $\rho_{33}$  versus intensity cannot be less than two for any classical

field with Gaussian statistics, where  $(N, M)$  specify the field correlation functions as defined in Ref. [10]. In the absence of atomic saturation, a similar result can be obtained from the analytic expressions Eqs. (21) and (23) of Ref. [10], as well as from numerical integrations of the master equation appropriate to our experiment. Various classical models based on pulsed excitation can likewise be excluded by demanding that the overall flux be constrained to that arising from intracavity photon numbers below unity for the OPO. By contrast our measurements are of slope  $\delta < 2$  extending into a region with  $\delta \sim 1.3$ . We thus conclude that our observations of two-photon excitation with squeezed light access a new regime in atomic spectroscopy whereby interactions with manifestly quantum or nonclassical fields lead to phenomena of a character not heretofore accessible.

We acknowledge support by the Division of Chemical Sciences, Office of Basic Energy Sciences, Office of Energy Research, U.S. Department of Energy and A. S. P. from the A. von Humboldt Foundation and the New Zealand Foundation for Research, Science, and Technology.

\*Permanent address: Aarhus University, Aarhus, Denmark.

†Permanent address: Tohoku University, Sendai, Japan.

‡Present address: University of Waikato, Hamilton, NZ.

- [1] R. Loudon, Rep. Prog. Phys. **43**, 913 (1980).
- [2] M. D. Teich and B. E. A. Saleh, in *Progress in Optics*, edited by E. Wolf (North Holland, Amsterdam, 1988), Vol. XXVI, pp. 1–104.
- [3] *Quantum Noise Reduction in Optical Systems*, edited by C. Fabre and E. Giacobino, Appl. Phys. B **55**, 189 (1992).
- [4] E. S. Polzik, J. Carri, and H. J. Kimble, Phys. Rev. Lett. **68**, 3020 (1992); Ref. [3], p. 279.
- [5] C. W. Gardiner, Phys. Rev. Lett. **56**, 1917 (1986).
- [6] A. S. Parkins, in *Modern Nonlinear Optics*, edited by M. Evans and S. Kielich (J. Wiley, New York, 1993), Vol. 2, pp. 607–666.
- [7] B. R. Mollow, Phys. Rev. **175**, 1555 (1968).
- [8] J. Janszky and Y. Yushin, Phys. Rev. A **36**, 1288 (1987).
- [9] J. Gea-Banacloche, Phys. Rev. Lett. **62**, 1603 (1989); J. Javanainen and P. L. Gould, Phys. Rev. A **41**, 5088 (1990).
- [10] Z. Ficek and P. D. Drummond, Phys. Rev. A **43**, 6247 (1992); **43**, 6258 (1992).
- [11] N. Ph. Georgiades, E. S. Polzik, and H. J. Kimble, Opt. Lett. **19**, 1474 (1994).
- [12] Note that while the data in Fig. 2(a) are for the direct output of the OPO with varying pump power to the OPO, the data in (b) are acquired in a separate experiment by injecting a coherent signal beam at  $\omega_{12}$  into the OPO for fixed gain  $G = 4$ . The resulting signal and idler fields pass through an attenuator [not present in (a)] of transmission coefficient  $10^{-3}$  with  $R_{1,2}$  varied by changing the power of the original injected beam.
- [13] C. Gardiner and A. S. Parkins, Phys. Rev. A **50**, 1792 (1994).